





# A DNA Vaccine Expressing Consensus Hemagglutinin-Esterase Fusion Protein Protected Guinea Pigs from Infection by Two Lineages of Influenza D Virus

Yanmin Wan,<sup>a,b</sup> Guobin Kang,<sup>a,b</sup> Chithra Sreenivasan,<sup>c</sup> Lance Daharsh,<sup>a,b</sup> Junfeng Zhang,<sup>a,b</sup> Wenjin Fan,<sup>a,b</sup>  Dan Wang,<sup>c,d</sup> Hideaki Moriyama,<sup>b</sup> Feng Li,<sup>c,d</sup>  Qingsheng Li<sup>a,b</sup>

<sup>a</sup>Nebraska Center for Virology, University of Nebraska—Lincoln, Lincoln, Nebraska, USA

<sup>b</sup>School of Biological Sciences, University of Nebraska—Lincoln, Lincoln, Nebraska, USA

<sup>c</sup>Department of Biology and Microbiology, South Dakota State University, Brookings, South Dakota, USA

<sup>d</sup>Department of Veterinary and Biomedical Sciences, South Dakota State University, Brookings, South Dakota, USA

**ABSTRACT** Two lineages of influenza D virus (IDV) have been found to infect cattle and promote bovine respiratory disease complex, one of the most commonly diagnosed causes of morbidity and mortality within the cattle industry. Furthermore, IDV can infect other economically important domestic livestock, including pigs, and has the potential to infect humans, which necessitates the need for an efficacious vaccine. In this study, we designed a DNA vaccine expressing consensus hemagglutinin-esterase fusion (HEF) protein (FluD-Vax) and tested its protective efficacy against two lineages of IDV (D/OK and D/660) in guinea pigs. Animals that received FluD-Vax ( $n = 12$ ) developed appreciable titers of neutralizing antibodies against IDV lineage representatives, D/OK and D/660. Importantly, vaccinated animals were protected against intranasal challenge with IDV [ $3 \times 10^5$  50% tissue culture infective dose(s) (TCID<sub>50</sub>)] D/OK ( $n = 6$ ) or D/600 ( $n = 6$ ), based on the absence of viral RNA in necropsied tissues (5 and 7 days postchallenge) using quantitative reverse transcription-PCR and *in situ* hybridization. In contrast, animals that received a sham DNA vaccine ( $n = 12$ ) had no detectable neutralizing antibodies against IDV, and viral RNA was readily detectable in respiratory tract tissues after intranasal challenge ( $3 \times 10^5$  TCID<sub>50</sub>) with IDV D/OK ( $n = 6$ ) or D/660 ( $n = 6$ ). Using a TUNEL (terminal deoxynucleotidyltransferase-mediated dUTP-biotin nick end labeling) assay, we found that IDV D/OK and D/600 infections induced apoptosis in epithelial cells lining alveoli and bronchioles, as well as nonepithelial cells in lung tissues. Our results demonstrate for the first time that the consensus IDV HEF DNA vaccine can elicit complete protection against infection from two lineages of IDV in the guinea pig model.

**IMPORTANCE** Influenza D virus (IDV) infection has been associated with bovine respiratory disease complex, one of the most devastating diseases of the cattle population. Moreover, with broad host range and high environmental stability, IDV has the potential to further gain virulence or even infect humans. An efficacious vaccine is needed to prevent infection and stop potential cross-species transmission. In this study, we designed a DNA vaccine encoding the consensus hemagglutinin-esterase fusion (HEF) protein of two lineages of IDV (D/OK and D/660) and tested its efficacy in a guinea pig model. Our results showed that the consensus DNA vaccine elicited high-titer neutralizing antibodies and achieved sterilizing protection against two lineage-representative IDV intranasal infections. To our knowledge, this is the first study showing that a DNA vaccine expressing consensus HEF is efficacious in preventing different lineages of IDV infections.

Received 18 January 2018 Accepted 2 March 2018

Accepted manuscript posted online 7 March 2018

**Citation** Wan Y, Kang G, Sreenivasan C, Daharsh L, Zhang J, Fan W, Wang D, Moriyama H, Li F, Li Q. 2018. A DNA vaccine expressing consensus hemagglutinin-esterase fusion protein protected guinea pigs from infection by two lineages of influenza D virus. *J Virol* 92:e00110-18. <https://doi.org/10.1128/JVI.00110-18>.

**Editor** Stacey Schultz-Cherry, St. Jude Children's Research Hospital

**Copyright** © 2018 American Society for Microbiology. All Rights Reserved.

Address correspondence to Qingsheng Li, [qli@unl.edu](mailto:qli@unl.edu).

**KEYWORDS** influenza D virus, hemagglutinin-esterase-fusion protein, consensus sequence, DNA vaccine, guinea pigs

Influenza D virus (IDV) has recently been classified as a new genus within the *Orthomyxoviridae* family and is distinct from influenza A, B, and C viruses (IAV, IBV, and ICV, respectively) (1, 2). IDV infects economically important domestic livestock, including swine and cattle, and has been associated with a respiratory disease/influenza-like illness (3–5). Furthermore, IDV seroprevalence in humans was estimated to be approximately 1.3% in the general population and over 90% in individuals working with cattle (6). These initial studies suggest that IDV may be able to infect humans, although its pathogenicity to humans remains unknown.

IDV has a broad host range. IDV was initially isolated from clinically ill pigs expressing influenza-like symptoms in 2011 (4). However, subsequently epidemiological data suggest cattle are the primary reservoir (1, 5, 7, 8). In addition to swine and cattle, IDV infections have been reported in goats, sheep, equines, buffalos, and camels (2, 5, 9, 10). IDV has also been shown to infect ferrets (4) and guinea pigs (11, 12) in experimental settings. IDV infections are widely distributed across many countries in the American, Asian, European, and African continents (1, 3, 13). Two lineages of IDVs were found to be cocirculating in the United States (3, 9). Recently, a potential third lineage of IDV was identified in Japan (14). IDV, like other influenza viruses, is a single-strand, negative-sense segmented and enveloped RNA virus. Both IAV and IBV have eight genomic segments and two surface glycoproteins of hemagglutinin (HA) and neuraminidase (NA). IDV, like ICV, has only seven genomic segments and one spike hemagglutinin-esterase fusion (HEF) protein (15, 16). The HEF combines the functions of HA and NA for receptor binding, receptor destruction, and membrane fusion activity (15, 16). While the overall structure of IDV HEF is similar to ICV, IDV HEF has an open receptor binding cavity to accommodate diverse extended glycan moieties, which may be one of the reasons for its broad host range (15).

IDV causes only mild or no obvious clinical symptoms in infected animals (2). However, it is thought to be a facilitating factor for the development of bovine respiratory disease complex (BRDC), which is one of the most commonly diagnosed causes of morbidity and mortality within the cattle industry (17). An efficacious preventative vaccine may be needed to protect economically important domestic animals and limit potential cross-species transmission to humans. To this end, we developed a DNA vaccine expressing consensus IDV HEF and tested its protective efficacy against two lineages of IDV using a guinea pig model. The consensus DNA vaccine elicited high-titer neutralizing antibodies and achieved sterilizing protection against two lineage-representative IDV intranasal infections in the guinea pig model, while all the animals in the control group were infected. This study demonstrates that a DNA vaccine-expressing consensus HEF is efficacious in preventing different lineages of IDV infections.

## RESULTS

**Phylogenetic and antigenic analysis of consensus IDV HEF protein.** IDV is similar to ICV in that it uses only one HEF spike for receptor binding, receptor destruction, and membrane fusion (18). The surface HEF thus represents a key protective immunogen for the development of a preventive vaccine. Two lineages of IDVs are primarily responsible for current IDV global infections (1, 3, 13). Furthermore, these two distinct lineages of IDVs can also coinfect the same animals (3, 19). To develop an IDV vaccine that could prevent infection from both lineages of IDV, we designed and constructed an IDV HEF consensus gene (ConD-HEF)-based vaccine, FluD-Vax. Phylogenetic analysis showed that the amino acid sequence of ConD-HEF resembles both lineages but is closer to the lineage represented by strain D/swine/Oklahoma/1334/2011 (D/OK) than the lineage represented by strain D/bovine/Oklahoma/660/2013 (D/660) (Fig. 1). The phylogenetic distance (average substitutions per amino acid) of ConD-HEF to D/OK is 0.5%, and that

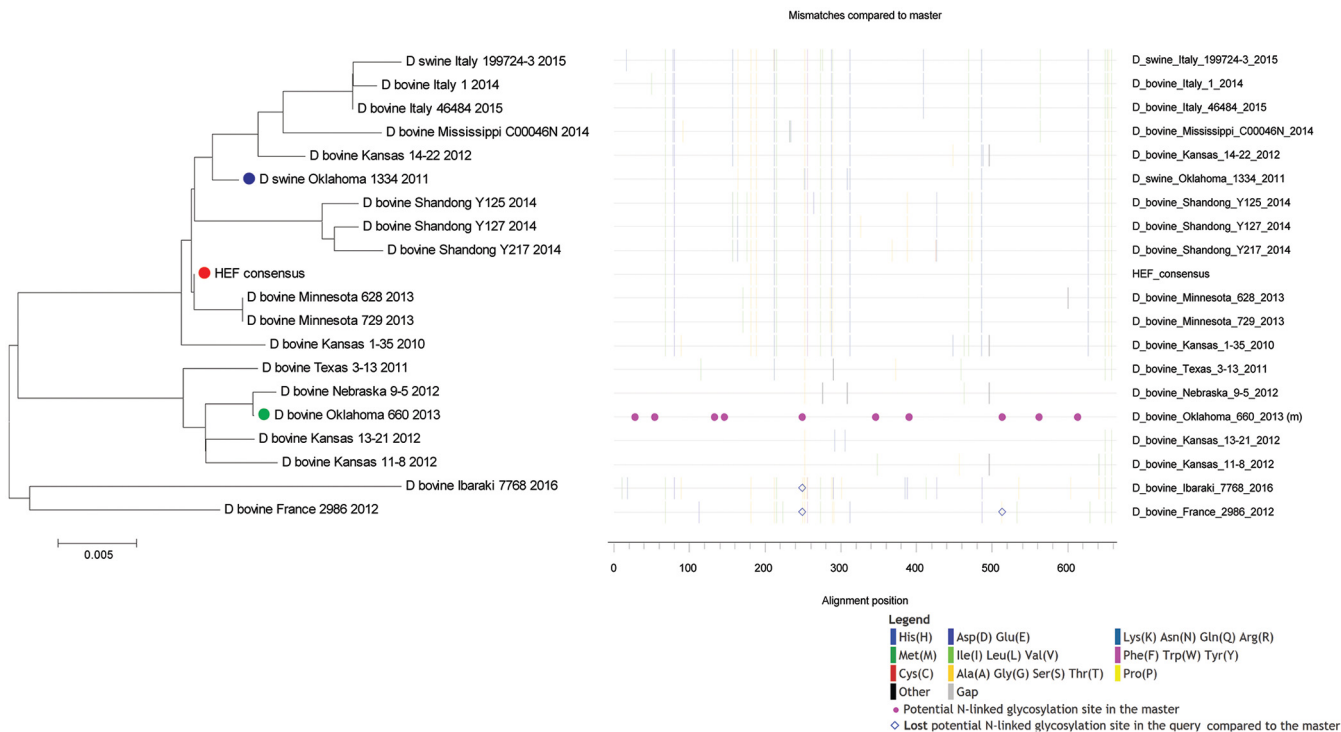


**FIG 1** Phylogenetic analysis of ConD-HEF protein. The phylogenetic relationship of HEF amino acid sequences between consensus vaccine (ConD-HEF) and 19 IDVs isolates was illustrated in a neighbor-joining phylogeny plot (left panel) and a highlighter plot (right panel). In the phylogeny plot, the consensus HEF is depicted as a closed red circle, D/swine/Oklahoma/1334/2011 (D/OK) as an open blue circle, and D/bovine/Oklahoma/660/2013 (D/660) as an open green circle. The scale bar length represents 0.005 amino acid substitutions per site. Amino acid polymorphisms in the highlighter plot are indicated by a colored mark.

to D/660 is 2.6%. The antigenicity of the consensus HEF protein expressed by the FluD-Vax was assessed by Western blotting. Our data showed that both the full-length HEF and the cleaved HEF1 (16) could be recognized by rabbit anti-IDV sera (data not shown).

**FluD-Vax elicited robust HI antibody responses against both D/OK and D/660 lineages.** As illustrated in Table 1, the guinea pigs in the vaccine and control groups were immunized with FluD-Vax or control plasmid DNA, respectively, four times at 4-week intervals. Peripheral blood was collected 3 weeks after each vaccination for evaluation of HEF-specific neutralizing antibodies against D/OK and D/660 using a hemagglutination inhibition (HI) assay. The HI antibody titers against both IDVs increased significantly after the second immunization and peaked after the third immunization. The mean titer of HI antibodies against D/OK was higher than that against D/660 after each vaccine immunization (Fig. 2A and B). Control groups did not generate a detectable HI antibody response at any time point (data not shown). Interestingly, after the final vaccination, the mean HI antibody titers to D/OK or D/660 between the

**TABLE 1** Guinea pig vaccination schedule

Group (n)	Treatment				
	Wk 0	Wk 4	Wk 8	Wk 12	Wk 16
Vac1 (6)	ConD HEF, 200 µg each	ConD HEF, 200 µg each	ConD HEF, 200 µg each	ConD HEF, 200 µg each	Challenge with IDV D/OK, 3 × 10 <sup>5</sup> TCID <sub>50</sub> /300 µl
Ctr1 (6)	Mock, 200 µg each	Mock, 200 µg each	Mock, 200 µg each	Mock, 200 µg each	Challenge with IDV D/OK, 3 × 10 <sup>5</sup> TCID <sub>50</sub> /300 µl
Vac2 (6)	ConD HEF, 200 µg each	ConD HEF, 200 µg each	ConD HEF, 200 µg each	ConD HEF, 200 µg each	Challenge with IDV D/660, 3 × 10 <sup>5</sup> TCID <sub>50</sub> /300 µl
Ctr2 (6)	Mock, 200 µg each	Mock, 200 µg each	Mock, 200 µg each	Mock, 200 µg each	Challenge with IDV D/660, 3 × 10 <sup>5</sup> TCID <sub>50</sub> /300 µl

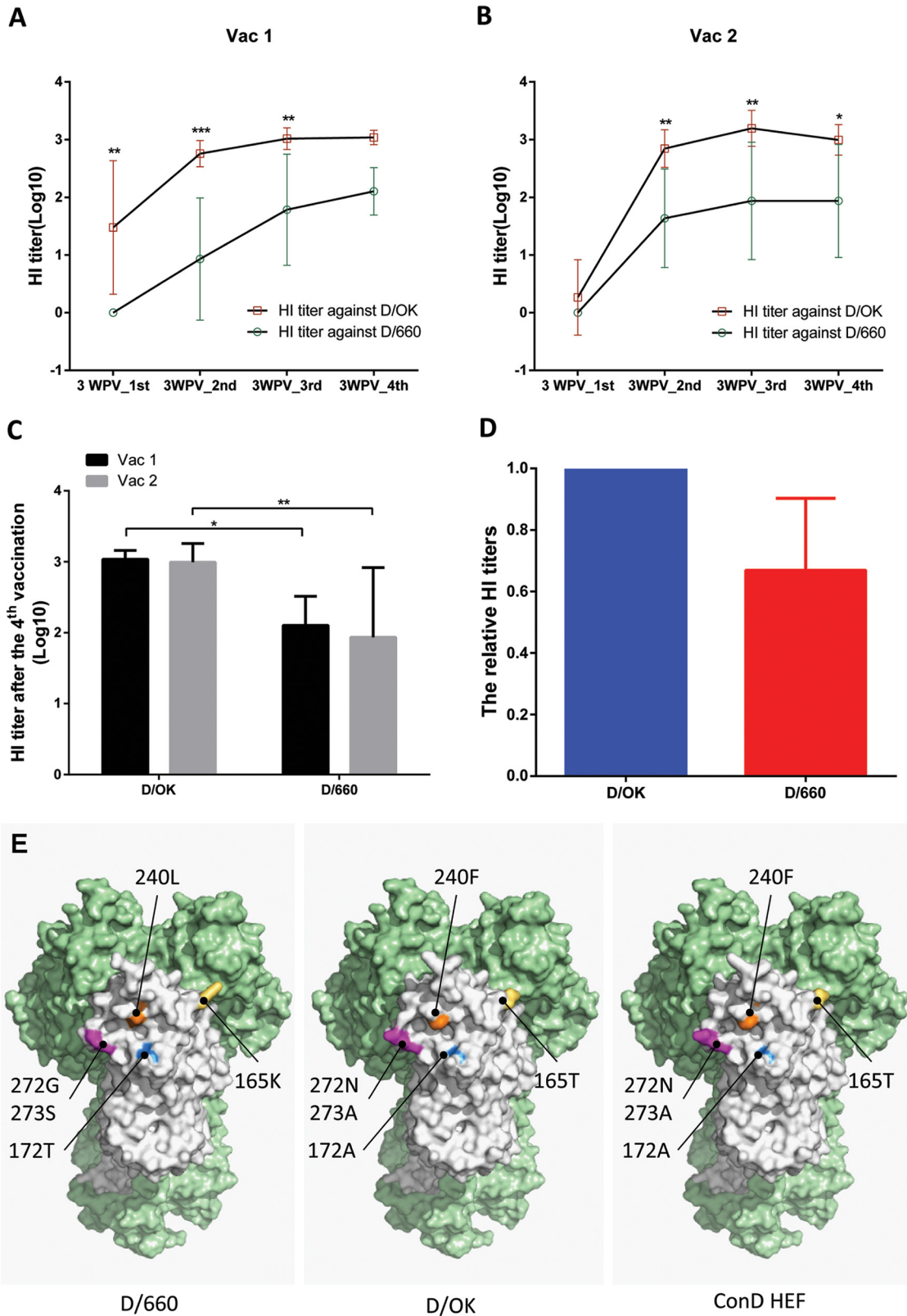


**FIG 2** HI antibody titers against D/OK and D/660 and structural comparisons among D/660, D/OK, and ConD HEF. Antibody responses in peripheral blood induced by ConD-HEF vaccine were evaluated by an HI assay. ConD-HEF vaccine induced robust HI antibody responses against D/OK and D/660 in both vaccine groups (A, Vac 1; B, Vac 2). However, the mean magnitudes against D/OK were higher than against D/660 over the course of immunization (\*,  $P < 0.05$ ; \*\*,  $P < 0.01$ ; \*\*\*,  $P < 0.001$ ). (C) The mean HI antibody titers of the two vaccine groups were very similar at 3 weeks after the final vaccination. (D) The relative HI titers were calculated by (Continued on next page)

two vaccine groups (Vac 1 and Vac 2) were similar (Fig. 2C), indicating that our vaccine induced a similar level of immune responses between the Vac 1 and Vac 2 groups. In addition, we also calculated the relative HI antibody titers of D/660 to D/OK and found that the mean ratio of D/660 versus D/OK HI titers was 0.67 (Fig. 2D).

**Efficacy of FluD-Vax protection against IDV infections.** To evaluate the protective efficacy of consensus FluD-Vax vaccine against two lineages of IDV infection, the guinea pigs in the Vac 1 and control 1 (Ctr 1) groups were challenged with IDV D/OK, and the Vac 2 and Ctr 2 groups were challenged with IDV D/660. A minimal loss of body weight (<5% on average) after viral challenge occurred in all groups, with a slightly greater reduction in body weight observed in the vaccine group after D/OK challenge compared to the control group (data not shown). The body temperatures of animals in both vaccine and control groups remained stable without significant fluctuation (data not shown).

To measure IDV infection, quantitative reverse transcription-PCR (qRT-PCR) and *in situ* hybridization (ISH) were used to detect viral RNA in respiratory tract tissues collected from euthanized animals. Most IDV quantitative real-time PCR assays were designed based on the originally isolated PB1 sequence (4). Recently, Faccini et al. improved this assay by targeting the primers and probe to the highly conserved segment of PB1 (20). Like PB1, the nucleoprotein (NP) gene is another conserved gene in influenza viruses, including IDV, which has been a primary target for RT-PCR assay development. The new method developed in our study can serve as an alternative to the RT-PCR assay targeting the PB1 gene, as published previously. In addition, there were other reasons for us to develop the current NP gene-based real-time PCR method. We did not have the PB1 standard used in the aforementioned assay; therefore, we developed an NP gene-based real-time PCR method. High viral loads were readily detected using qRT-PCR in all the lung tissues of guinea pigs from both control groups immunized with a sham vaccine and challenged with either D/OK or D/660 IDV. The mean viral RNA load in the D/OK control group (mean  $\pm$  the standard deviation,  $7.41 \pm 0.81$ ,  $\log_{10}$ ) was significantly higher than in the D/660 control group ( $5.52 \pm 2.52$ ,  $\log_{10}$ ) (Fig. 3). In contrast, no IDV viral RNA was detected in any lung tissues from the vaccine groups immunized with FluD-Vax and challenged with either D/OK or D/660 IDV (Fig. 3). To investigate whether IDV exists in peripheral blood in IDV infected animals, we conducted qRT-PCR and found that one animal was IDV positive in plasma ( $3.09 \times 10^4$  copies/ml). The animal with IDV-positive plasma was infected with D/OK and had the highest viral load in lung tissues ( $3.16 \times 10^8$  copies/ $\mu$ g of total RNA), indicating that IDV from the respiratory tract can spread into peripheral blood if the IDV virus burden is very high. However, none of any other animals in the vaccine and control groups had detectable IDV RNA in plasma. To confirm qRT-PCR results, we detected viral RNA in respiratory tract tissues collected from euthanized animals using ISH. Consistent with the qRT-PCR results, ISH confirmed that all of the animals in the control groups were infected after IDV intranasal challenge, as evidenced by the presence of abundant IDV vRNA-positive cells in respiratory tract tissues, such as in the lungs (Fig. 4) and in nasal turbinate and tracheal tissues (Fig. 5). The presence of IDV vRNA-positive cells in nasal turbinate, septum, trachea, and lung tissues further confirmed that IDV can infect both the upper and lower respiratory tracts. Of note, IDV has a predisposition to infect the lungs (Fig. 4 and 5). As shown in Fig. 4 and 5, both lineage representative IDVs infected bronchioles and the alveoli of lung tissues, with more vRNA<sup>+</sup> cells found in bronchioles than in alveoli. As expected, we did not find IDV-infected cells in the draining lymph node tissues of the lungs. Pan-cytokeratin

#### FIG 2 Legend (Continued)

normalizing the D/660 HI titer to the D/OK HI titer for each individual animal. Error bars represent the standard deviations. (E) The HEF protein structure of influenza D virus (Protein Data Bank [PDB] accession no. 5E64) was selected as the template, and all models received a QMEAN value of  $-0.45$ . The trimer formation was determined versus the HEF protein structure of influenza C virus (PDB accession no. 1FLC). One subunit is white, while the other two are light green. Graphics were prepared using the PyMOL Molecular Graphics System (v1.8; Schrödinger, LLC, New York, NY).



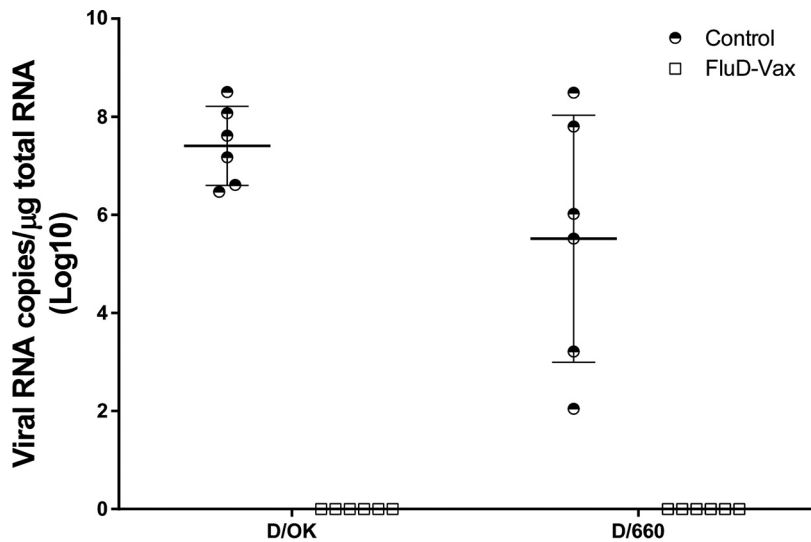


**FIG 3** IDV RNA load in lung tissues quantified using qRT-PCR. No IDV viral RNA was detected in any lung tissues of vaccinated animals challenged with either D/OK or D/660 IDV, whereas viral RNA was detected in all control animals.

immunohistochemical staining in combination with ISH confirmed that the IDV-infected cells were epithelial cells (Fig. 6).

**IDV infection caused apoptosis in lung tissues.** To determine whether IDV infection could cause programmed cell death in lung tissues, we conducted TUNEL (terminal deoxynucleotidyltransferase-mediated dUTP-biotin nick end labeling) assays on lung tissues from all of the animals in the vaccine and control groups. We detected apoptotic cells in lung tissues on days 5 and 7 after IDV D/660 (Fig. 7C to F) and D/OK (Fig. 7I to L) infection in animals from the control groups. TUNEL-positive cells were mainly localized in the epithelial cells lining alveoli (Fig. 7C, E, I, and K, black arrows) and bronchioles (Fig. 7D, F, H, and L, black arrows within blue circles). However, TUNEL-positive cells were also detected in nonepithelial cells (Fig. 7, green arrows). In contrast, we did not observe TUNEL-positive cells in animals from the vaccine group (Fig. 7A, B, G, and H).

## DISCUSSION

The newly identified influenza D virus (IDV) has been demonstrated to infect economically important domestic livestock, such as swine and cattle. IDV infection has been reported to be significantly associated with bovine respiratory disease complex (BRDC) (21, 22), which is the most economically significant disease affecting the U.S. cattle industry. While the level of infectivity and pathogenicity of IDV to humans remains to be determined, IDV has the potential to infect humans. IDV seroprevalence was estimated to be over 90% in individuals working closely with cattle (7). Moreover, IDV has a broad host range (2), which could enable IDV to gain virulence due to continual mutation, recombination, and evolution (5).

The development of a protective IDV vaccine is needed. However, the development of an effective vaccine is not simple, since a previous study showed that a chemical inactivated IDV vaccine did not provide sterilizing protection against even homologous virus challenge in bovine (23). As mentioned previously, two genetically and serologically distinct lineages of IDV have been found to be cocirculating in cattle (3) and equines (9). Therefore, we sought to develop a vaccine that could prevent infection by both lineages of IDV. Use of a consensus sequence-based vaccine is a widely used approach to minimize the sequence diversity between a vaccine strain and circulating viruses, which can create an artificial sequence to “centralize” the immunogenicity of the vaccine antigen (24–26). In addition to the consensus sequence-based vaccine

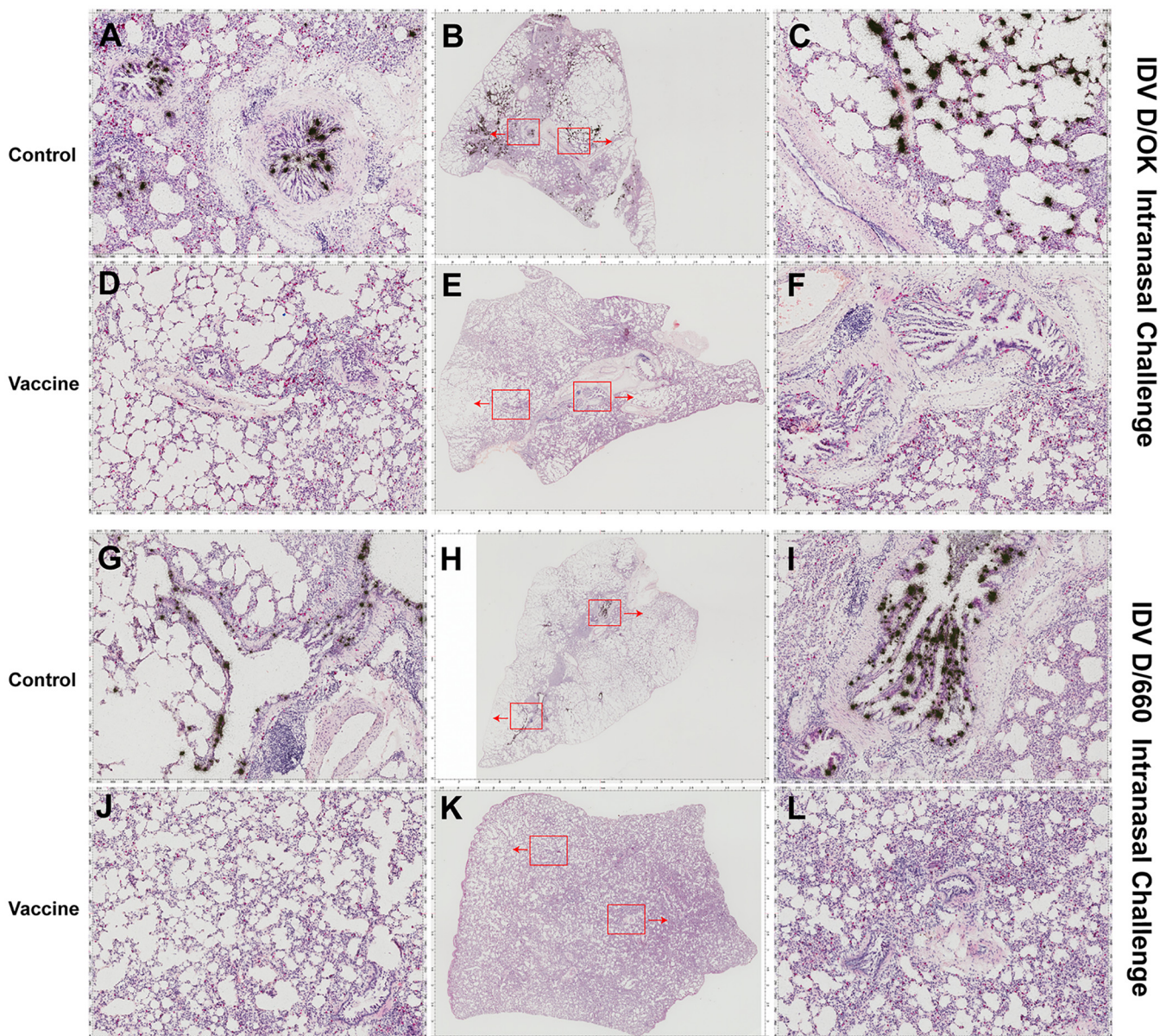


**FIG 4** IDV RNA<sup>+</sup> cells in lung tissues detected using ISH. IDV RNA<sup>+</sup> cells (black silver grains in radioautographs) were detected in all of the lung tissues of animals who received the sham vaccine (control) and subsequently challenged intranasally with IDV D/OK (A to C, animal 1084) or D/660 (G to I, animal 1091) but were not detected in any lung tissues of animals who received the FluD-Vax vaccine and subsequently challenged with IDV D/OK (D to F, animal 1099) or D/660 (J to L, animal 1106). Red insets in the middle panel are magnified and shown in the left and right panels.

development approach, “ancestor” and “center of the tree” methods have also been applied to minimize the distance/mismatch of antigens between a vaccine and circulating viruses. As previously reported (26), when designing a consensus vaccine from the sequences of a symmetric phylogeny, these three methods generate very similar sequences. However, if the original sequences are from an asymmetric phylogeny, the consensus sequence will have a bias toward the dominant cluster of the input. In this study, we designed and constructed a DNA vaccine encoding a consensus IDV HEF protein (ConD-HEF). The HEF surface protein was chosen for its key role in receptor binding, receptor destruction, and membrane fusion. Phylogenetic analysis showed that ConD-HEF is close to the center of the IDV phylogenetic tree, with a slight bias toward the lineage represented by D/OK (Fig. 1). We did not do further optimization to reduce this bias because in a natural infection, D/OK could generate relatively more



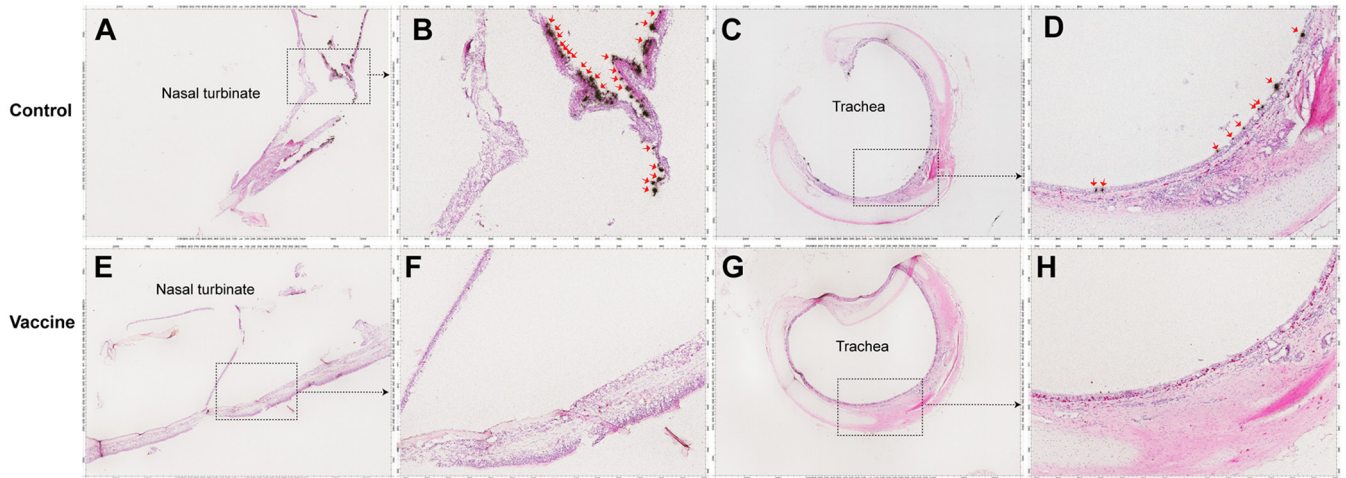


**FIG 5** IDV RNA<sup>+</sup> cells in nasal turbinate and tracheal tissues detected using ISH. Representative images show that no IDV RNA<sup>+</sup> cells (black silver grains in radioautographs, red arrows) were detected in any nasal turbinate (E and F, animal 1099) and tracheal tissues (G and H, animal 1099) of animals who received the FluD-Vax vaccine and were subsequently challenged with IDV D/OK or D/660. IDV RNA<sup>+</sup> cells (black silver grains in radioautographs) were detected in nasal turbinate (A and B, animal 1084) and tracheal tissues (C and D, animal 1099) of control animals who received the sham vaccine and were subsequently challenged with IDV D/OK or D/660. Insets are magnified in images marked by shown arrows.

highly cross-reactive antibodies to D/660 represented lineage than D/660 to D/OK (3). In this study, 19 full-length IDV HEFs were used for the consensus vaccine design, including the 10 sequences that were previously analyzed for the identification of the two major circulating lineages (D/OK and D/660) (3). For future vaccine design, the inclusion of additional viral sequences, especially sequences that isolated from different geographic locations, may further optimize the coverage of a consensus DNA IDV vaccine.

Our previous study established a guinea pigs/IDV model (12). With this model, we

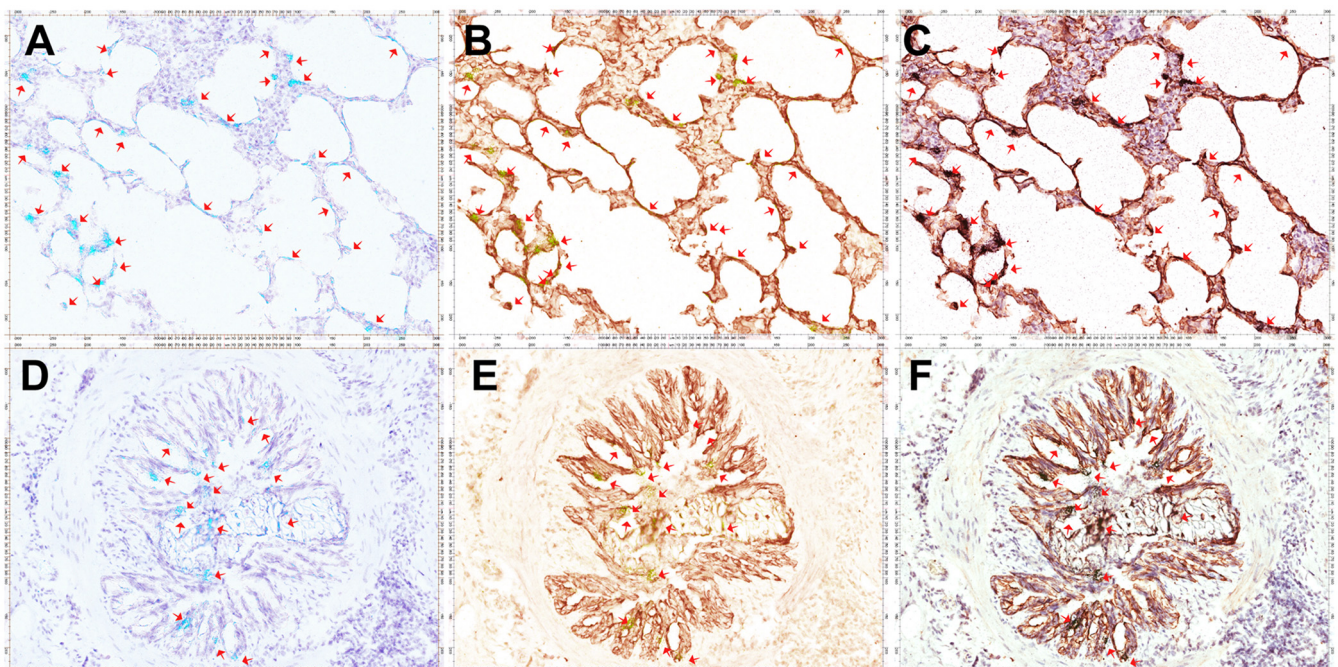


**FIG 6** IDV-infected cell types in control group IDV challenged lung tissues determined using combined IHCS and ISH. Representative images show epithelial cells in lung tissues that were immunohistochemically stained as brown (brown in panels B, C, E, and F, animal 1084) with a pan-cytokeratin antibody and IDV RNA underlaid of silver grains in radioautographs as cyan, yellow, or black (red arrows) with different channel separation.



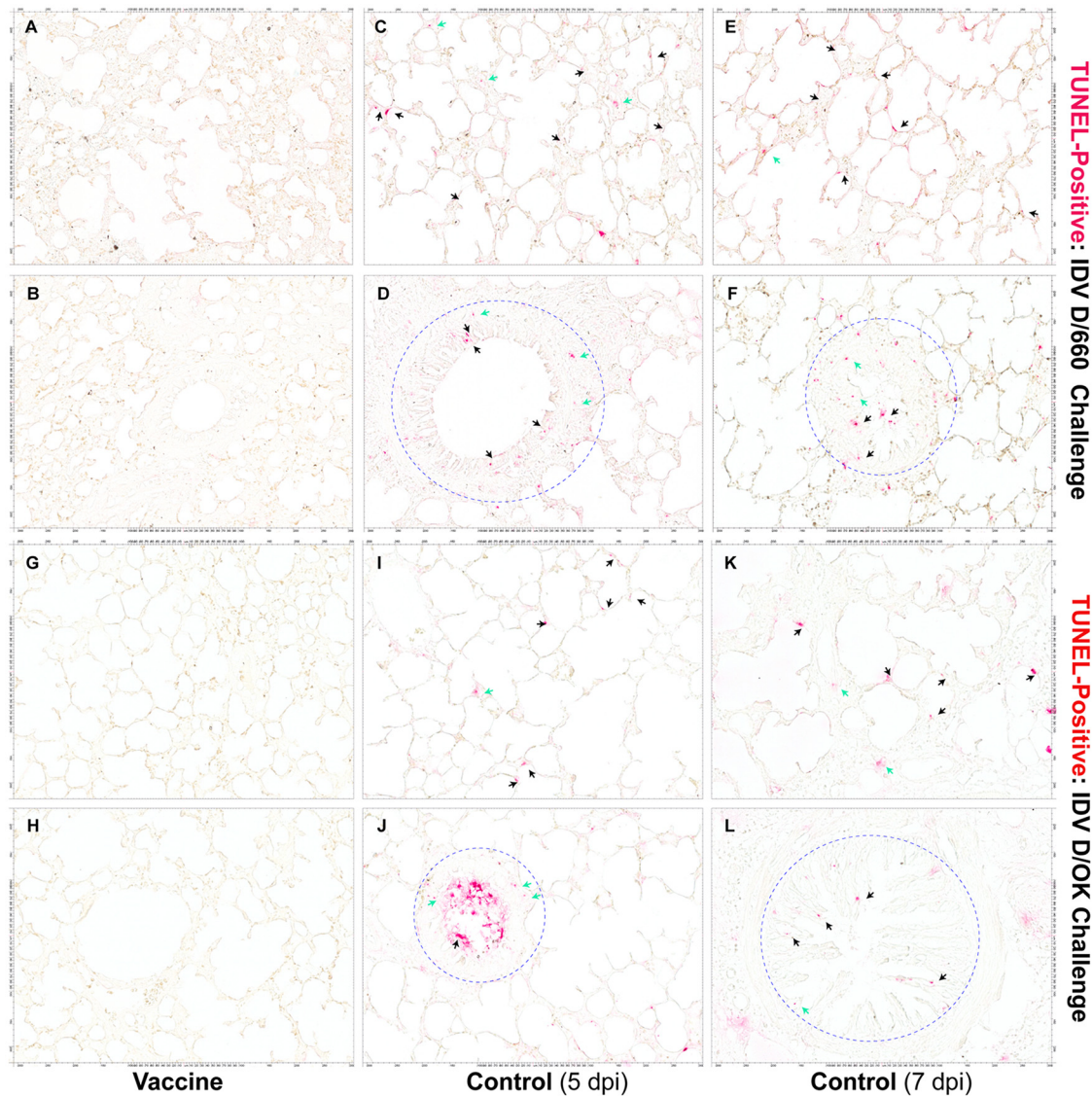


**FIG 7** Micrographs of apoptotic cells in IDV-infected lung tissues detected with a TUNEL assay. TUNEL-positive epithelial cells lining alveoli (C, E, I, and K; red; black arrows) and bronchioles (D, F, H, and L; red; black arrows within blue circles) and non-epithelial cells (red, green arrows) in lung tissues were detected in all animals who received the sham vaccine (control) and subsequently challenged intranasally with IDV D/660 (C to F) or D/OK (I to L) but were not detected in animals who received the FluD-Vax vaccine and subsequently challenged with IDV D/660 (A and B) or IDV D/OK (G and H). Scale bars are shown on four sides of the image panels.

first evaluated humoral immune responses elicited by the consensus HEF DNA vaccine (FluD-Vax). HI antibodies in blood against both D/OK and D/660 IDVs were detectable after the first immunization, were significantly boosted after the second immunization ( $>1:40$ ), and peaked after the third immunization (Fig. 2A and B). In this proof-of-concept study, in order to induce optimal humoral responses and achieve better protection, we immunized the animals four times. However, sterilizing protection may be induced by fewer than four immunizations, and future studies are needed to determine the minimal number of immunizations to achieve sterilizing protection. We observed more robust HI antibody responses against D/OK than against D/660 (Fig. 2), which may be due to the intentional phylogenetic bias design of our consensus vaccine to D/OK. We also performed *in silico* comparative modeling of D/OK, D/660, and ConD HEF protein structures by the SWISS-MODEL server (27) and found several amino acid substitutions in the receptor binding site of D/660 HEF (Fig. 2E). Although our consensus DNA vaccine elicited various levels of HI antibodies against D/OK and D/660, it

protected all vaccinated animals from IDV D/OK and D/660 intranasal challenge, indicating that the vaccine-elicited immunity is potent enough to protect against both lineages of IDV infection (Fig. 3 to 5). In contrast, all animals in the control groups were infected after IDV challenge.

After D/OK and D/660 challenge, infected animals in the control groups had higher viral RNA loads in respiratory tissues at 5 days postinfection than at 7 days postinfection, as determined by both the qRT-PCR and the ISH assays, which is consistent with our previous study (12). IDV RNA<sup>+</sup> cells were detected in nasal turbinate, nasal septum, trachea, and lung tissues, indicating that IDV can infect and replicate within the entire respiratory tract. Notably, within lung tissues, viral RNA<sup>+</sup> cells were detected in both alveoli and bronchioles, but more in bronchiolar cells. Using a combination of immunohistochemical staining (IHCS) and ISH, we showed that IDV solely infected epithelial cells. Although the exact protective mechanisms of our consensus vaccine against prevalent lineages of IDV infection was not fully investigated in this study, our results revealed that protection is correlated with HI antibody responses. One concern during IDV vaccine design is the potential for escape mutations that could minimize protection. However, the DNA vaccine expressing consensus IDV HEF in this study provided complete protection and prevented the occurrence of IDV escape mutations. However, IDV mutations can readily develop during IDV natural infection; thus, a broad understanding of potentially mutated antigenic sites in IDV vaccine design is important.

Although the protection observed in guinea pigs cannot be directly translated to cattle or human protection due to potential biological differences, our data suggested that the consensus HEF may be a good immunogen to protect against different lineages of IDV in large animals or even in humans. Further investigation is warranted to compare its efficacy with other vaccine modalities, such as inactivated and vectored vaccines.

Currently, the pathogenesis and resulting consequences of IDV infection in economically important animals are largely unknown. Apoptosis has been demonstrated to be an important antiviral host defense to restrict influenza A and B virus replication. Paradoxically, apoptosis has also been implicated in inducing respiratory tissue damage during influenza virus infection (18, 28, 29). Until this study, it remained unknown whether IDV infection results in apoptosis in the respiratory tract. We found for the first time that IDV infection induced TUNEL-positive apoptotic cells in epithelial cells lining alveoli (Fig. 7C, E, I, and K, black arrows) and bronchioles (Fig. 7D, F, H, and L, black arrows within blue dotted circles) in lung tissues of infected animals. Furthermore, we observed TUNEL-positive nonepithelial cells (Fig. 7, green arrows). Our results demonstrate that IDV infection can cause apoptosis in lung tissues. Nevertheless, the dichotomy of protective and detrimental roles of apoptosis during IDV infection remains to be defined in future studies.

In summary, our study has demonstrated that a DNA vaccine expressing consensus IDV HEF can provide complete protection, which is correlated with HEF-specific antibody responses in a guinea pig model. Further, our study clearly demonstrated that IDV infects epithelial cells of both the upper and lower respiratory tracts, including alveoli and bronchioles in lung tissues. More importantly, we found for the first time that IDV infection can induce programmed cell death in lung tissues.

## MATERIALS AND METHODS

**Animals and animal procedures.** Guinea pig experiments were conducted by following the protocol approved by the Institutional Animal Care and Use Committees at University of Nebraska—Lincoln (UNL). Twenty-four specific-pathogen-free or viral-antibody-free ~3-month-old female guinea pigs of the Dunkin-Hartley strain (Elm Hill Labs, Chelmsford, MA) were used in this study. The animals were individually housed and were ear tagged after a 1-week acclimation period.

**Consensus DNA vaccine design and preparation.** To develop a vaccine that could prevent both lineages of IDV infection, a consensus HEF DNA vaccine was designed. The HEF amino acid sequences of 19 IDVs isolated between 2011 and 2016 were downloaded from GenBank, from which the consensus sequence (664 amino acids) was calculated using BioEdit (v7.2.0). Codons of the consensus HEF gene were optimized for efficient expression in mammalian cells by using an online tool (JCat [<http://www.jcat.de/>]). After codon optimization, the consensus HEF gene was synthesized (GENEWIZ LLC, South

**TABLE 2** Primers and probe for real-time PCR

Oligonucleotide	Sequence (5'-3')	Positions (nt) <sup>a</sup>
NP_forward	AAGCGACGTTCCAAGAAGCTG	1542–1561
NP_reverse	GGGACTGCAACAGAACCATC	1716–1697
NP_probe	FAM-TGCTCCGGCACCTTGCTTCC-TAMRA	1647–1627

<sup>a</sup>Numbering is from the sequence of the D/swine/Oklahoma/1334/2011 NP gene (accession number [JQ922306](#)). nt, nucleotides.

Plainfield, NJ) and inserted into the pJW4303 expression vector, which was kindly provided by Shan Lu (University of Massachusetts Medical School, Worcester, MA). The constructed plasmid with the HEF insert was designated FluD-Vax, and the same plasmid without the HEF insert was used as a vector control. FluD-Vax and control plasmid DNA were prepared by using an EndoFree Plasmid Giga kit (catalog no. 12391; Qiagen, Germany) for guinea pig vaccination.

**Experiment design.** Guinea pigs were randomly divided into four groups (six per group). Animals in the vaccine groups (Vac 1 and Vac 2) were each inoculated in tibialis anterior muscle with FluD-Vax (200  $\mu$ g/animal) four times at 4-week intervals, and animals in the control groups (Ctr 1 and Ctr 2) were each inoculated with the same quantity of control plasmid DNA in parallel. A detailed vaccination schedule is shown in Table 1.

**IDV challenge and sample collection.** To test the protective efficacy of FluD-Vax against two lineages of IDV, animals in the Vac 1 and Ctr 1 groups were challenged with an IDV D/OK lineage-representative strain (D/swine/Oklahoma/1334/2011 [D/OK]), and animals in the Vac 2 and Ctr 2 groups were challenged with a D/660 lineage-representative strain (D/bovine/Oklahoma/660/2013 [D/660]) (Table 1). IDV stocks were prepared as previously reported (12) and diluted in phosphate-buffered saline (PBS) containing 100 U/ml penicillin, 100  $\mu$ g/ml streptomycin, and 0.3% bovine serum albumin (PBS-PS-BA). A 300- $\mu$ l volume of IDV inoculum containing  $3 \times 10^5$  50% tissue culture infective dose(s) (TCID<sub>50</sub>) was instilled into the nostrils (150  $\mu$ l on each side) at 30 days after the final immunization. After IDV challenge, each animal's head and nose were kept slightly elevated with respect to the rump for 15 min to prevent the inoculum from flowing out of the nostrils.

Body weight and temperature of the guinea pigs were monitored daily for up to 7 days starting from the day of IDV challenge before virus inoculation (day 0). At 5 and 7 days postchallenge, two and four animals from each group were euthanized, respectively. Immediately after euthanasia, blood, nasal turbinate, septum, soft palate, trachea, lung, and draining lymph node samples were collected. Half of the collected tissues were fixed in 4% paraformaldehyde, and the remaining half were snap-frozen immediately in liquid nitrogen.

**IDV HI assay.** Guinea pig sera were treated with receptor-destroying enzyme (RDE; Denka Seiken, Tokyo, Japan) before the HI assay was performed. The RDE treatment was performed according to the manufacturer's protocol, and the HI assay was performed according to our previously described method (12). The HI assay was performed against the two representative IDV-lineage viruses (D/swine/Oklahoma/1334/2011 and D/bovine/Oklahoma/660/2013) using 1% turkey red blood cells (Lampire Biological Laboratories, Pipersville, PA).

**Real-time qRT-PCR.** Primers and probe were designed to target a conserved region of the NP gene (Table 2). A recombinant plasmid containing the full-length NP sequence of the IDV strain D/swine/Oklahoma/1334/2011 (accession number [JQ922306](#)) was serially diluted and used as a qRT-PCR standard. Snap-frozen lung tissue was put into a 2-ml tube prefilled with stainless steel beads (RNA-WIST01; WISBIOMED LLC, San Mateo, CA) and homogenized for 2 min using a MiniBeadBeater-16 (BioSpec Products, Inc., Bartlesville, OK). RNA from homogenized lung tissues and plasma specimens was extracted using a QIAamp viral RNA minikit (catalog no. 52906; Qiagen). The qRT-PCR was performed in 20  $\mu$ l containing  $1 \times$  TaqMan Fast Virus 1-Step master mix (catalog no. 4444434; Thermo Fisher Scientific, Waltham, MA), 500 nM concentrations of each primer, a 250 nM concentration of probe, and 5  $\mu$ l of total RNA extracted from supernatants of homogenized guinea pig lung tissues. The cycling conditions were as follows: reverse transcription step at 50°C for 5 min, followed by an RT inactivation/initial denaturation step at 95°C for 20 s, 45 cycles of denaturation at 95°C for 3 s, and annealing/extension at 60°C for 30 s. The fluorescence signal was detected after the annealing/extension step at each cycle. All PCR assays were performed on a CFX96 real-time PCR system (Bio-Rad, Hercules, CA). The lower limit of detection for this method was verified to be  $\sim 10$  copies/reaction (data not shown).

**ISH.** IDV in respiratory tract tissues was detected using *in situ* hybridization (ISH) with radioactive isotopes of sulfur (<sup>35</sup>S)-labeled negative-sense RNA probes of HEF and nucleoprotein (NP). HEF (1,071 bp) and NP (1,024 bp) cDNA templates were amplified from D/OK HEF and NP gene plasmids using PCR with the following primer pairs containing polymerase sequences: (i) HEF-forward primer-T7 (AACGTGTAATACGACTACTATAGGG and AGGGGCTTCGTTGATGTTGT) and HEF reverse primer-SP6 (AACTGGATTAGG TGACTATAG and AAGATCCTTGTGCTGGCGT) and (ii) NP-forward primer-T7 (AACGTGTAATACGACTACTATAGGG and TGGCAAGCAAAAAGAACGGG) and NP-reverse primer-SP6 (AACTGGATTAGGTGACACTATAGG and CCTCTTTCTTGGGCTGGGA). Negative-sense riboprobes from HEF and NP were generated by *in vitro* runoff transcription with SP6 RNA polymerase and used for the detection of viral transcripts. Tissue sections (6  $\mu$ m) were cut, and ISH was conducted according to our previously published method (30). Slides were exposed for 3 days in radioautography and counterstained with hematoxylin and eosin. Tissue sections were digitized using a ScanScope (Nikon), and IDV RNA positivity was reviewed by two investigators independently. The specificity of the IDV riboprobes was confirmed using HIV-1 riboprobes as a negative-control probe and rhesus lung tissues as negative-control tissues.



**Combined IHCS and ISH.** To determine the cell type of IDV-infected cells, a combination of IHCS and ISH was performed as previously described (31). A pan-cytokeratin rabbit polyclonal antibody (MA5-13203, 1:150; Invitrogen) and diaminobenzidine, along with the Dako Envision and peroxidase kit, were used for IHCS. Stained tissue sections were digitized using a ScanScope, and the viral RNA ISH signal and IHC-stained epithelial cell signal were viewed in a single-color channel and combined color channels using Aperio's Spectrum Plus analysis program (v9.1; Aperio ePathology Solutions).

**In situ cell death detection by TUNEL assay.** To detect apoptotic cell death in lung tissues, a TUNEL assay was performed as previously described (31). *In situ* cell death detection AP kit (catalog no. 11-684 809 910; Roche) and AP substrate (RNAscope 2.0 HD detection kit; RED, ACD) were used to immunohistochemically detect TUNEL-positive apoptotic cells as red color signals. The stained tissue sections were digitized using a ScanScope.

**Statistical analysis.** Statistical analyses were performed using GraphPad Prism 6.0 (GraphPad Software, La Jolla, CA). The HI antibody titers of the two groups at multiple time points were compared by two-way analysis of variance. Data are presented as means  $\pm$  the standard deviations in Fig. 2 and 3. A *P* value of  $<0.05$  was considered statistically significant.

## ACKNOWLEDGMENTS

Q.L. and Y.W. conceived the idea and designed the overall experiments with F.L. Y.W. designed and prepared the vaccine. Y.W., G.K., L.D., J.Z., and W.F. conducted the animal experiments. C.S. and D.W. prepared the virus stocks and measured the HI antibody titers. G.K. and J.F. conducted the ISH. Y.W. conducted the qRT-PCR. H.M. did the structural modeling of HEF protein receptor sites. Y.W. and Q.L. wrote the manuscript, and all authors commented and made revisions.

We thank Shan Lu for providing pJW4303 expression vector and staff members at the Institutional Animal Care Program of UNL for assistance in animal care.

This project was funded in part by start-up funds from UNL, grants SDSU AES 3AH-477 and NIH R21AI107379, National Science Foundation/EPSCoR (<http://www.nsf.gov/od/iaa/programs/epscor/index.jsp>) award IIA-1335423, and the state of South Dakota Governor's Office of Economic Development as a South Dakota Research Innovation Center.

## REFERENCES

- Hause BM, Collin EA, Liu R, Huang B, Sheng Z, Lu W, Wang D, Nelson EA, Li F. 2014. Characterization of a novel influenza virus in cattle and swine: proposal for a new genus in the *Orthomyxoviridae* family. *mBio* 5:e00031-14. <https://doi.org/10.1128/mBio.00031-14>.
- Su S, Fu X, Li G, Kerlin F, Veit M. 2017. Novel Influenza D virus: epidemiology, pathology, evolution, and biological characteristics. *Virulence* 8:1580-1591. <https://doi.org/10.1080/21505594.2017.1365216>.
- Collin EA, Sheng Z, Lang Y, Ma W, Hause BM, Li F. 2015. Cocirculation of two distinct genetic and antigenic lineages of proposed influenza D virus in cattle. *J Virol* 89:1036-1042. <https://doi.org/10.1128/JVI.02718-14>.
- Hause BM, Ducatez M, Collin EA, Ran Z, Liu R, Sheng Z, Armien A, Kaplan B, Chakravarty S, Hoppe AD, Webby RJ, Simonson RR, Li F. 2013. Isolation of a novel swine influenza virus from Oklahoma in 2011 which is distantly related to human influenza C viruses. *PLoS Pathog* 9:e1003176. <https://doi.org/10.1371/journal.ppat.1003176>.
- Zhai SL, Zhang H, Chen SN, Zhou X, Lin T, Liu R, Lv DH, Wen XH, Wei WK, Wang D, Li F. 2017. Influenza D virus in animal species in Guangdong Province, southern China. *Emerg Infect Dis* 23:1392-1396. <https://doi.org/10.3201/eid2308.170059>.
- White SK, Ma W, McDaniel CJ, Gray GC, Lednicky JA. 2016. Serologic evidence of exposure to influenza D virus among persons with occupational contact with cattle. *J Clin Virol* 81:31-33. <https://doi.org/10.1016/j.jcv.2016.05.017>.
- Ducatez MF, Pelletier C, Meyer G. 2015. Influenza D virus in cattle, France, 2011-2014. *Emerg Infect Dis* 21:368-371. <https://doi.org/10.3201/eid2102.141449>.
- Ferguson L, Eckard L, Epperson WB, Long LP, Smith D, Huston C, Genova S, Webby R, Wan XF. 2015. Influenza D virus infection in Mississippi beef cattle. *Virology* 486:28-34. <https://doi.org/10.1016/j.virol.2015.08.030>.
- Nedland H, Wollman J, Sreenivasan C, Quast M, Singrey A, Fawcett L, Christopher-Hennings J, Nelson E, Kaushik RS, Wang D, Li F. 2017. Serological evidence for the cocirculation of two lineages of influenza D viruses in equine populations of the Midwest United States. *Zoonoses Public Health* 65:e148-e154. <https://doi.org/10.1111/zph.12423>.
- Salem E, Cook EAJ, Lbacha HA, Oliva J, Awoume F, Aplogan GL, Hymann EC, Muloi D, Deem SL, Alali S, Zouagui Z, Fevre EM, Meyer G, Ducatez MF. 2017. Serologic evidence for influenza C and D virus among ruminants and camelids, Africa, 1991-2015. *Emerg Infect Dis* 23:1556-1559. <https://doi.org/10.3201/eid2309.170342>.
- Mubareka S, Lowen AC, Steel J, Coates AL, Garcia-Sastre A, Palese P. 2009. Transmission of influenza virus via aerosols and fomites in the guinea pig model. *J Infect Dis* 199:858-865. <https://doi.org/10.1086/597073>.
- Sreenivasan C, Thomas M, Sheng Z, Hause BM, Collin EA, Knudsen DEB, Pillatzki A, Nelson E, Wang D, Kaushik RS, Li F. 2015. Replication and transmission of the novel bovine influenza D virus in a guinea pig model. *J Virol* 89:11990-12001. <https://doi.org/10.1128/JVI.01630-15>.
- Sheng Z, Ran Z, Wang D, Hoppe AD, Simonson R, Chakravarty S, Hause BM, Li F. 2014. Genomic and evolutionary characterization of a novel influenza-C-like virus from swine. *Arch Virol* 159:249-255. <https://doi.org/10.1007/s00705-013-1815-3>.
- Murakami S, Endoh M, Kobayashi T, Takenaka-Uema A, Chambers JK, Uchida K, Nishihara M, Hause B, Horimoto T. 2016. Influenza D virus infection in herd of cattle, Japan. *Emerg Infect Dis* 22:1517-1519. <https://doi.org/10.3201/eid2208.160362>.
- Song H, Qi J, Khedri Z, Diaz S, Yu H, Chen X, Varki A, Shi Y, Gao GF. 2016. An open receptor-binding cavity of hemagglutinin-esterase-fusion glycoprotein from newly identified influenza D virus: basis for its broad cell tropism. *PLoS Pathog* 12:e1005411. <https://doi.org/10.1371/journal.ppat.1005411>.
- Wang M, Veit M. 2016. Hemagglutinin-esterase-fusion (HEF) protein of influenza C virus. *Protein Cell* 7:28-45. <https://doi.org/10.1007/s13238-015-0193-x>.
- Murray GM, O'Neill RG, More SJ, McElroy MC, Earley B, Cassidy JP. 2016. Evolving views on bovine respiratory disease: an appraisal of

- selected key pathogens. *Vet J* 217:95–102. <https://doi.org/10.1016/j.tvjl.2016.09.012>.
18. Ludwig S, Pleschka S, Planz O, Wolff T. 2006. Ringing the alarm bells: signaling and apoptosis in influenza virus infected cells. *Cell Microbiol* 8:375–386. <https://doi.org/10.1111/j.1462-5822.2005.00678.x>.
  19. Nedland H, Wollman J, Sreenivasan C, Quast M, Singrey A, Fawcett L, Christopher-Hennings J, Nelson E, Kaushik RS, Wang D, Li F. 2018. Serological evidence for the cocirculation of two lineages of influenza D viruses in equine populations of the Midwest United States. *Zoonoses Public Health* 65:e148–e154. <https://doi.org/10.1111/zph.12423>.
  20. Faccini S, De Mattia A, Chiapponi C, Barbieri I, Boniotti MB, Rosignoli C, Franzini G, Moreno A, Foni E, Nigrelli AD. 2017. Development and evaluation of a new real-time RT-PCR assay for detection of proposed influenza D virus. *J Virol Methods* 243:31–34. <https://doi.org/10.1016/j.jviromet.2017.01.019>.
  21. Mitra N, Cernicchiaro N, Torres S, Li F, Hause BM. 2016. Metagenomic characterization of the virome associated with bovine respiratory disease in feedlot cattle identified novel viruses and suggests an etiologic role for influenza D virus. *J Gen Virol* 97:1771–1784. <https://doi.org/10.1099/jgv.0.000492>.
  22. Ng TF, Kondov NO, Deng X, Van Eenennaam A, Neibergs HL, Delwart E. 2015. A metagenomics and case-control study to identify viruses associated with bovine respiratory disease. *J Virol* 89:5340–5349. <https://doi.org/10.1128/JVI.00064-15>.
  23. Hause BM, Huntimer L, Falkenberg S, Henningson J, Lechtenberg K, Halbur T. 2017. An inactivated influenza D virus vaccine partially protects cattle from respiratory disease caused by homologous challenge. *Vet Microbiol* 199:47–53. <https://doi.org/10.1016/j.vetmic.2016.12.024>.
  24. Chen MW, Cheng TJ, Huang Y, Jan JT, Ma SH, Yu AL, Wong CH, Ho DD. 2008. A consensus-hemagglutinin-based DNA vaccine that protects mice against divergent H5N1 influenza viruses. *Proc Natl Acad Sci U S A* 105:13538–13543. <https://doi.org/10.1073/pnas.0806901105>.
  25. Laddy DJ, Yan J, Corbitt N, Kobinger GP, Weiner DB. 2007. Immunogenicity of novel consensus-based DNA vaccines against avian influenza. *Vaccine* 25:2984–2989. <https://doi.org/10.1016/j.vaccine.2007.01.063>.
  26. Nickle DC, Jensen MA, Gottlieb GS, Shriner D, Learn GH, Rodrigo AG, and Mullins JI. 2003. Consensus and ancestral state HIV vaccines. *Science* 299:1515–1518.
  27. Kiefer F, Arnold K, Kunzli M, Bordoli L, Schwede T. 2009. The SWISS-MODEL repository and associated resources. *Nucleic Acids Res* 37:D387–D392. <https://doi.org/10.1093/nar/gkn750>.
  28. Brydon EWA, Morris SJ, Sweet C. 2005. Role of apoptosis and cytokines in influenza virus morbidity. *FEMS Microbiol Rev* 29:837–850. <https://doi.org/10.1016/j.femsre.2004.12.003>.
  29. Tripathi S, Batra J, Cao W, Sharma K, Patel JR, Ranjan P, Kumar A, Katz JM, Cox NJ, Lal RB, Sambhara S, Lal SK. 2013. Influenza A virus nucleoprotein induces apoptosis in human airway epithelial cells: implications of a novel interaction between nucleoprotein and host protein Clusterin. *Cell Death Dis* 4:e562. <https://doi.org/10.1038/cddis.2013.89>.
  30. Li Q, Gebhard K, Schacker T, Henry K, Haase AT. 1997. The relationship between tumor necrosis factor and human immunodeficiency virus gene expression in lymphoid tissue. *J Virol* 71:7080–7082.
  31. Li Q, Duan L, Estes JD, Ma ZM, Rourke T, Wang Y, Reilly C, Carlis J, Miller CJ, Haase AT. 2005. Peak SIV replication in resting memory CD4<sup>+</sup> T cells depletes gut lamina propria CD4<sup>+</sup> T cells. *Nature* 434:1148–1152. <https://doi.org/10.1038/nature03513>.